AIAA-94-3760-CP

# AN ANALYTICAL APPROACH FOR CONTINUOUS-THRUST, LEO-GEO TRANSFERS

by

David B. Spencer *
Phillips Laboratory, New Mexico
and
Robert D. Culp**
University of Colorado, Boulder



## Abstract

This paper examines an analytical method to transfer a spacecraft from a Low-Earth Orbit (LEO), circular and inclined to the equator, to a Geosynchronous Earth Orbit (GEO), with no inclination or eccentricity, in an analytical, near-optimal fashion. The focus is to examine the propulsive mass cost for a continuously thrusting vehicle, specifically, to develop a method to simplify the trajectory optimization problem for this type of vehicle.

The complexities of this problem are such that an analytical study is difficult to accomplish. Simplifications and approximations that are acceptable for some type of problems are limited by the assumptions made. Analytical approximations work for many cases, such as very low-thrust, where perturbation methods can approximate the small change in the orbital elements quite well. On the other end of the thrust spectrum, impulsive approximations (infinite thrust, infinitely small duration) can also yield valid results. In between, for intermediate-level thrust, neither small perturbation methods nor infinitely small thrust duration approximation is valid. For very low-thrust levels, both analytical and numerical solutions are acceptably close. Likewise, for the impulsive thrust burn, analytical and numerical results compare favorably. Numerical approaches can yield valuable results for the entire thrust level spectrum, but existing software tends to lack robustness, and are generally computationally intensive.

The method used in this paper to reduce the computational burden is to simplify the problem. The goal, just like the true optimization problem, is to transfer from one orbit to another, by expending the minimal amount of propellant. The sum of the duration of all burn-arcs and coast-arcs is the total transfer time.

The first burn arc in the transfer is designed so as to maximize the time rate in change in apogee radius. Once the apogee radius reaches the GEO altitude, the coast arc begins. This coast arc continues until the spacecraft reaches a radius that the time rate of change in perigee is maximized. Then, the second burn arc begins. The pointing direction of the thrust vector is determined so as to keep the apogee radius constant, and increases the perigee radius until it reaches the same value as the apogee radius. For a plane change, the most efficient use of mass occurs when the velocity is a minimum, and the vector is pointed perpendicular to the orbit plane. Additionally, a variation of the thrust-to-mass ratios was studied, and the effects of this parameter on the mass cost were then determined.

The results showed that an analytical LEO-GEO transfer can be accomplished using the techniques presented range from 1% of the optimal cost for high-thrust transfers, down 2.5% of the optimal cost for an intermediate to low-thrust transfer. This makes this technique a good first estimate algorithm of an optimal solution.

## Introduction

The problem to be examined in the course of this paper will be that of determining the near-optimal orbit transfer characteristics of a continuously thrusting propulsion system, and comparing it to the

---

* Orbital Dynamics Program Manager, Space and Missiles Dynamics Division, Phillips Laboratory, Senior Member, AIAA, Member, AAS. Address: PL/VTA, 3550 Aberdeen Avenue SE, Kirtland AFB, NM, 87117-5776.

* Professor and Chairman, Department of Aerospace Engineering Sciences, Associate Fellow, AIAA, Fellow, AAS. Address: Campus Box 429, Boulder, CO 80309-0429.

optimal orbit transfer. In the design phase, sizing of the system occurs, and the value of having a simple method to determine the near-optimal cost is very important. The methods presented here are further detailed in references [4] and [5].

The transfer begins with a burn arc that changes the apogee of the initial orbit to a geosynchronous radius. The perigee is allowed to increase during that burn arc, as well. Once the transfer orbit's apogee is at the geosynchronous altitude, a coast arc begins. As the spacecraft reaches the apogee radius, a plane change maneuver begins. This plane change is most efficient when the velocity is smallest, so the orbit plane is rotated to the final inclination. In the cases where the plane change burn arc is of significant duration, the burn arc is spread out over the apogee passage, for example, if it takes the spacecraft 10 seconds total to rotate the plane, then the plane change begins 5 seconds before apogee passage, and ends 5 seconds after apogee passage. A velocity threshold can also be implemented when the initial thrust-to-mass ratio is low, and it takes multiple revolutions to complete. After the inclination has reached its final value, the orbit is then recircularized. The recircularization is accomplished by increasing the perigee radius, while keeping the apogee radius constant. When the instantaneous radius approaches the instantaneous perigee radius, a coast arc is initiated. This is because at the perigee radius, the perigee radius cannot be raised faster than the instantaneous radius increases. For the low initial thrust-to-mass ratios, it may take several small burn arcs, separated by several small coast arcs, to accomplish this recircularization.

## Analysis

The natural dynamical equations of motion in an inverse-square gravitational field, with a perturbation vector in the form of a propulsive force are now presented in equinoctial coordinates. The concept of eccentricity and inclination control using a Fourier series analysis is presented next. The initial estimation of the associated Fourier coefficients for the eccentricity and inclination control is then derived. Next, several control laws are developed for the LEO-GEO transfer.

Any element set can be used. Earth-Centered-Inertial (ECI) $(x, y, z, \dot{x}, \dot{y}, \dot{z})$ are easily implemented, but show little insight into the behavior of the system. Classical elements, $(a, e, i, \Omega, \omega, M)$ give good physical insight on the system, but prove difficult for low eccentricity, and low inclination orbits. Equinoctial elements [1] eliminate several of the singularities of the classical elements, and prove useful for the specific cases to be studied. Because of this, the equinoctial orbital elements are used for the analysis throughout the course of this paper. The geometry of the equinoctial coordinate frame is shown in Figure 1.

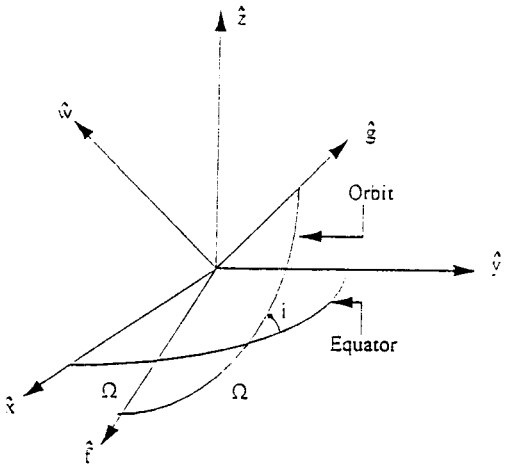


Figure 1: Geometry of Coordinate Frame

Here, these equations of motion are presented in matrix form, as:

$$\frac{dX}{dt} = \frac{T}{m(t)} M\hat{u} + n\zeta \qquad [1]$$

where

$$X = (a \quad h \quad k \quad p \quad q \quad \lambda)^T,$$

M=6x3 matrix,

$$\hat{u} = \begin{pmatrix} u_f \\ u_g \\ u_w \end{pmatrix},$$

$$\zeta = (0 \quad 0 \quad 0 \quad 0 \quad 0 \quad 1)^T$$

and the mass flow equation is:

$$\frac{dm(t)}{dt} = -\left(\frac{T}{c}\right) \qquad [2]$$

The elements of the M matrix are shown in the appendix. To eliminate the need for a value of mass, equation [2] is non-dimensionalized. Introducing the variable

$$\eta(t) = \frac{m(t)}{m_o} \qquad [3]$$

with the time derivative of $\eta$ being

$$\frac{d\eta}{dt} = \frac{1}{m_o}\frac{dm}{dt} \qquad [4]$$

equation [2] is then replaced by

$$\frac{d\eta}{dt} = -\left(\frac{T}{m_o}\right)\left(\frac{1}{c}\right) \qquad [5]$$

where $\frac{T}{m_o}$ is the initial thrust-to-mass ratio, and the ratio of $\frac{T}{m(t)}$ is replaced in equation [1] by $\frac{T}{m_o}\frac{1}{\eta(t)}$

**Eccentricity Control**

One way to solve this problem is to apply a forcing function on the eccentricity variable, and examine the effects of this control law on the other orbital elements. If the yaw angle of the transfer is designated by the angle α, and the pitch angle is designated by the angle, β, the control variables $u_f$, $u_g$ and $u_w$, in the equinoctial reference frame, become:

$$u_f = \cos\alpha\cos\beta \qquad [6]$$

$$u_g = \sin\alpha\cos\beta \qquad [7]$$

and

$$u_w = \sin\beta. \qquad [8]$$

The eccentricity is related to the equinoctial elements by

$$e = \sqrt{h^2 + k^2} \qquad [9]$$

Taking the time derivative of equation [9], yields

$$\frac{de}{dt} = \frac{1}{\sqrt{h^2+k^2}}\left(h\dot{h} + k\dot{k}\right) \qquad [10]$$

The method examined in this paper is to model the eccentricity as an infinite Fourier series. The sine and cosine functions have many desirable features. They are easily computed by rapidly convergent series. Their successive integrals and derivatives are again sines and cosines. Finally, they have orthogonality properties and are periodic. For the continuous eccentricity function, the trigonometric series is

$$e(t) = \frac{1}{2}a_0 + \sum_{n=1}^{\infty}\left(a_n\cos nt + b_n\sin nt\right) \qquad [11]$$

where

$$a_n = \frac{1}{P}\int_{-P}^{P} e(t)\cos\frac{n\pi t}{P}dt$$

and

$$b_n = \frac{1}{P}\int_{-P}^{P} e(t)\sin\frac{n\pi t}{P}dt$$

where P is the period of the oscillation.

Taking the time derivative of equation [11], and equating it to equation [10], a transcendental equation is formed,

$$\sum_{n=1}^{\infty} n(-a_n\sin nt + b_n\cos nt) = \frac{1}{e}\left[(hM_{21}+kM_{31})u_f + (hM_{22}+kM_{32})u_g + (hM_{23}+kM_{33})u_w\right] \qquad [12]$$

Substituting the expressions for the control vectors, a transcendental equation is found for the control angle α,

$$(hM_{21}+kM_{31})\cos\alpha + (hM_{22}+kM_{32})\sin\alpha = \frac{-(hM_{23}+kM_{33})\sin\beta + e\sum_{n=1}^{\infty} n(-a_n\sin nt + b_n\cos nt)}{\cos\beta} \qquad [13]$$

The coefficients can then be determined after modeling the eccentricity in any fashion desired.

The significance of equation [13] is that any eccentricity time history (including an optimal solution) can be modeled as a Fourier series approximation. If the eccentricity time history can be better described by another curve, such as a polynomial, least-squares, splines, or a straight line, the time derivative can be inserted in place of the summation in equation [13].

**Inclination Control**

The same principles can be applied to inclination control. Just as the yaw angle α controls the eccentricity, the pitch angle β controls the inclination. The relationship between the inclination and the equinoctial elements, p and q, is

$$i = 2\tan^{-1}\left(p^2+q^2\right)^{1/2} \qquad [14]$$

Taking the derivative of this equation with respect to time yields:

$$\frac{di}{dt} = \frac{2(p\dot{p}+q\dot{q})}{\left(p^2+q^2\right)^{1/2}\left(1+p^2+q^2\right)} \qquad [15]$$

Since the variables p and q are influenced by a change in the pitch angle, β, the inclination time history is independent of the yaw angle directly, and is only effected by the yaw angle indirectly, due to the yaw angle's effects the semimajor axis and the eccentricity. The inclination can be modeled in any way

desired, and just like the eccentricity, a Fourier series was chosen, as:

$$i(t) = \frac{1}{2}c_0 + \sum_{n=1}^{\infty}(c_n \cos nt + d_n \sin nt) \quad [16]$$

where the coefficients can be chosen to model the time history, as desired.

Taking the time derivative of equation [16], and equating it to equation [15], the approximate value of the pitch angle, β, becomes:

$$\beta = \sin^{-1}\left\{\frac{\left[\sum_{n=1}^{\infty} n(-c_n \sin nt + d_n \cos nt)\right]\tan\frac{i}{2}\sec^2\frac{i}{2}}{2(pM_{43} + qM_{53})}\right\} \quad [17]$$

In order to begin this analysis, initial sets of coefficients for eccentricity control and inclination control must be found. The dynamics of several control laws is presented, and the theory regarding the Fourier coefficient determination is applicable to any of the control laws used.

## Maximization of $\frac{da}{dt}$ Control Law; First Burn Arc in LEO-GEO Transfer

If there are no attitude constraints, a control law where the amount of energy put into the system is maximized can be used. This relatively simple control likewise maximizes the time rate of change in semimajor axis. The energy is found from the simple relation,

$$E = -\frac{\mu}{2a} \quad [18]$$

Taking the time derivative of equation [18], we get,

$$\frac{dE}{dt} = \frac{\mu}{2a^2}\frac{da}{dt}. \quad [19]$$

Thus, maximizing the time rate of change of energy is equivalent to maximizing the time rate of change of semimajor axis.

Expanding the first row of equation [1] (with the non-dimensional transformation on mass), and noting that $M_{13} = 0$ (from the appendix), becomes

$$\frac{da}{dt} = \left(\frac{T}{m_0}\right)\left(\frac{1}{\eta(t)}\right)[M_{11}\cos\alpha\cos\beta + M_{12}\sin\alpha\cos\beta] \quad [20]$$

Taking the partial derivative of equation [20] with respect to the control angle α, and assuming that cosβ is not equal to zero, setting the partial derivative equal to zero maximizes the time rate of change in semimajor axis, a (since the minimum value of equation [20] is 0). Doing this, the control law becomes:

$$\alpha = \tan^{-1}\left(\frac{M_{12}}{M_{11}}\right) \quad [21]$$

For many cases, it is not cost effective to have only one burn arc for the transfer. In these cases, a coast arc is inserted between two burn arcs. The point where the coast arc begins is determined from the control law used for the first burn. When the apogee radius reaches the apogee radius desired, the thrust is turned off.

## Plane Change Maneuver in a LEO-GEO Transfer Orbit

The same procedure for determining the velocity at which to perform an out-of-plane maneuver can be employed for a LEO-GEO transfer as well. When the position in the burn arc approaches the perigee radius, the perigee radius cannot be changed without increasing the apogee radius. Therefore, if the ratio of the instantaneous radius and the perigee is less than some threshold, say perhaps 1.01, the thrust is turned off, and a coast arc is instituted. This allows for a longer transfer time, but does not waste propellant. This situation occurs only when there are multiple perigee passes, which correspond to the lower thrust level simulations.

The plane change can be broken up based on the most efficient use of propellant. One way to break up the inclination change would be to begin the out-of-plane changes when the velocity of the spacecraft in the orbit falls below a given value, since the effective inclination change is more efficient when the velocity is smaller. The out-of-plane control law used in equation [17] can be used in this case as well. In all cases, it is necessary to iterate on where the out-of-plane maneuver begins. If the velocity threshold where the inclination change occurs is too high, then the inclination change will not be enough to reach the final desired value. If the velocity threshold is too low, the inclination will change too much.

## Recircularizing the Transfer Orbit

In going into the second burn arc, the goal is to change the perigee radius, while keeping the apogee radius constant. This can be done by examining the dynamics of the perigee radius. The radius at perigee $r_p$, is found as

$$r_p = a(1-e) \qquad [22]$$

Taking the time derivative of equation [22], the time rate of change in perigee radius is

$$\frac{dr_p}{dt} = -a\frac{de}{dt} + \frac{da}{dt}(1-e) \qquad [23]$$

In addition to changing the perigee radius, the apogee radius must remain constant. With the apogee radius, $r_a$, given as

$$r_a = a(1+e) \qquad [24]$$

and setting the time derivative equal to zero,

$$\frac{dr_a}{dt} = 0 = a\frac{de}{dt} + (1+e)\frac{da}{dt} \qquad [25]$$

the time derivative of semimajor axis can be solved for, as

$$\frac{da}{dt} = -\left(\frac{a}{1+e}\right)\frac{de}{dt} \qquad [26]$$

Inserting equation [26] into equation [23], the time derivative of perigee radius is

$$\frac{dr_p}{dt} = -\frac{2a}{1+e}\frac{de}{dt} \qquad [27]$$

Putting the previous equation into equinoctial elements, equation [27] becomes

$$\frac{dr_p}{dt} = -\frac{2a}{\left[\left(h^2+k^2\right)^{1/2} + h^2 + k^2\right]}\left(h\frac{dh}{dt} + k\frac{dk}{dt}\right) \qquad [28]$$

In order to obtain the control angle that keeps the apogee radius constant, we next take the partial derivative of equation [25] with respect to the control angle, $\alpha$, and setting it equal to zero, that control angle becomes

$$\alpha = \tan^{-1}\left\{\frac{\mp\left[hM_{21} + kM_{31} + \frac{e+e^2}{a}M_{11}\right]}{\pm\left[hM_{22} + kM_{32} + \frac{e+e^2}{a}M_{12}\right]}\right\} \qquad [29]$$

In order to determine whether to use the positive or negative value of $\alpha$, the second derivative test on equation [28] shows that, in order to attain a local maximum, the constraint

$$\frac{1}{\cos\alpha}(hM_{21} + kM_{31}) > 0 \qquad [30]$$

must be satisfied.

Short of a numerical optimization process, there is no simple way to determine the best way to perform a three-dimensional transfer where the orbit plane is changing at the same time as the shape of the planar orbit. However, some simplifications and assumptions can be made to allow for an easier solution procedure.

## Quality of the Solution

In order to study the quality of solutions, a measure of how good the coefficients perform must be determined. For the coplanar transfer, the *best* case (the one that requires the lowest amount of propellant) is the two-impulse Hohmann transfer. The impulsive change in velocity for the first burn is computed from the well-known equation:

$$\Delta v_1 = \sqrt{\frac{\mu}{r_p}}\left[\sqrt{\frac{2(r_a/r_p)}{1+(r_a/r_p)}} - 1\right] \qquad [31]$$

while the impulsive change in velocity for the second burn is

$$\Delta v_2 = \sqrt{\frac{\mu}{r_a}}\left[1 - \sqrt{\frac{2}{1+(r_a/r_p)}}\right] \qquad [32]$$

Relating the amount of $\Delta v_i$ (i=1,2) applied to the amount of mass used,

$$\Delta m_i = m_{i-1}\left[1 - e^{\left(\frac{-\Delta v_i}{g_o I_{sp}}\right)}\right] \qquad [33]$$

where:

$m_i \equiv$ *mass of spacecraft after* $i^{th}$ *burn*

For an inclination change maneuver, the $\Delta$v requirement is

$$\Delta v = 2v\sin\frac{\Delta i}{2} \qquad [34]$$

which corresponds to a mass cost of found in equation [33].

The cost is presented as a function of the specific impulse used. However, in order to eliminate the dependence on specific impulse, the cost can be changed into an "effective $\Delta$v". Integrating the mass ratio rate equation [5], yields

$$\sum_{i=0}^{N}\eta(t_{i+1}) - \eta(t_i) = -\left(\frac{T}{m_o}\right)\left(\frac{1}{g_o I_{sp}}\right)\sum_{i=0}^{N}\delta(t_{i+1} - t_i) \qquad [35]$$

where

$$\delta = \begin{cases} 1 & \textit{during burn arc} \\ 0 & \textit{during coast arc} \end{cases}$$

The mass ratio changes only during the burn arc, so equation [35] reduces to

$$\eta(t_f) - \eta(t_o) = -\left(\frac{T}{m_0}\right)\left(\frac{1}{g_0 I_{sp}}\right)\tau \qquad [36]$$

where $\tau$ is the total burn arc time duration. The term $\eta(t_o)$ is the mass ratio at the beginning of the burn arc, while the term $\eta(t_f)$ is the mass ratio at the end of the burn arc. Solving equation [36] for the specific impulse term, yields

$$\frac{1}{g_0 I_{sp}} = -\frac{\ln(\eta(t_f)) - \ln(\eta(t_o))}{\Delta v} \qquad [37]$$

Inserting equation [37] into equation [36], and solving for the effective $\Delta v$ gives,

$$\Delta v = -\left(\frac{T}{m_o}\right)\left(\frac{\ln \eta(t_f) - \ln(t_o)}{\eta(t_f) - \eta(t_o)}\tau\right) \qquad [38]$$

There has been various amounts of results published that give the "optimal" transfer parameters for a wide range of initial thrust-to-mass ratios. Each "optimal" case published has its own merits and limitations, and therefore is not used to gauge the results presented in this dissertation. The Hohmann transfer approximation is still the best gauge to judge the quality of the results for the high-thrust cases, while perturbation methods provide a good gauge to the low-thrust cases.

## Results

In this section, the transfer analyzed uses initial thrust-to-mass ratios ranging from very high (100,000 N/kg) to very low (0.01 N/kg). This transfer is a combination of orbit shape change and orbit plane change.

The simulation begins with a circular orbit, with a radius of 7,000 km, inclined to the orbit at 28.5°, and ends with a circular orbit with a radius of approximately 42,241 km, with zero inclination. For numerical approximations, the initial eccentricity is set at an arbitrarily small value, as is the final eccentricity and inclination. The locations of the spacecraft in the initial and final orbits are arbitrary, and are coupled, and are therefore not presented, except that the initial mean anomaly is chosen so that the first burn arc ends at an equatorial crossing.

The cases presented here have three major burn arcs (the second and third burn arcs are sequential, and are effectively one burn arc), and possibly some smaller burn arcs in the recircularization maneuver. In actual operations, the plane change and recircularization burns can be combined into one maneuver. This would reduce the impulsive cost by approximately 400 m/sec, and would likewise decrease the effective $\Delta v$ for all of the transfers presented here.

All of the small burn arcs in the recircularization are included in the effective $\Delta v$ for the recircularization. Table 1 shows the costs for this simulation for seven orders-of-magnitude in initial thrust-to-mass.

| $\frac{T}{m_o}\left(N/kg\right)$ | Effective $\Delta v$ for First Burn (m/sec) | Effective $\Delta v$ for Plane Change Burn (m/sec) | Effective $\Delta v$ for Re-circular-ization (m/sec) | Total Effective $\Delta v$ (m/sec) |
|---|---|---|---|---|
| 100,000 | 2338 | 810 | 1420 | 4568 |
| 10,000 | 2339 | 811 | 1419 | 4569 |
| 1,000 | 2339 | 814 | 1419 | 4572 |
| 100 | 2339 | 817 | 1419 | 4575 |
| 10 | 2341 | 819 | 1418 | 4578 |
| 1 | 2543 | 853 | 1352 | 4748 |
| 0.1 | 3785 | 1237 | 856 | 5878 |
| 0.01 | 4307 | 4549 | 153 | 9009 |
| 3 Impulse Approx.[1] | 2338 | 805 | 1425 | 4568 |

Table 1: Three-Dimensional, LEO-GEO Transfer Cost

Zondervan [6] and Redding [3] presented results for optimal LEO-GEO transfers. Since the initial conditions are not the same in the two references and this study, the transfer costs are normalized with respect to the individual impulsive costs, and are presented in Figure 2.

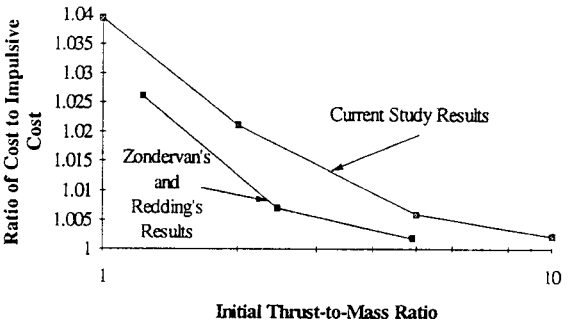


Figure 2: Comparison of Current Study Results to Zondervan and Redding

### LEO-GEO Fourier Approximation

A Fourier transformation is applied to the eccentricity time history for the first burn arc, the inclination time history for the plane change maneuver, and the remaining eccentricity time history for the recircularization maneuver in an example LEO-GEO

transfer. The eccentricity control portion of the transfer occurs during the two periods when the eccentricity is changing. The inclination control portion occurs when the inclination is changing.

## Eccentricity Control for First Burn Arc for LEO-GEO Transfer

The Fourier transformation is applied to an example eccentricity time history for the first burn arc. The superposition of the Fourier series approximation on the eccentricity time history allowed for creation of this figure., which was created using 317 Fourier coefficients (159 "a" coefficients, and 158 "b" coefficients).

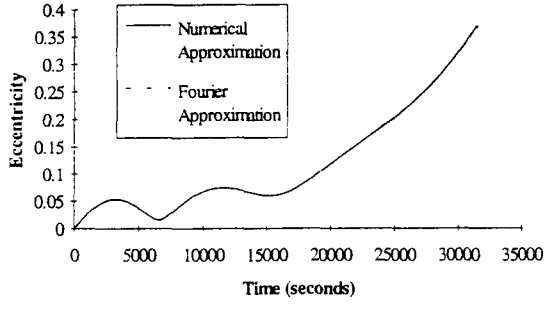


Figure 3: Eccentricity Time History with Fourier Series Approximation

The curves plotted in Figure 3 are nearly indistinguishable. To further discern these curves, the absolute value of the difference between these curves is plotted in Figure 4.

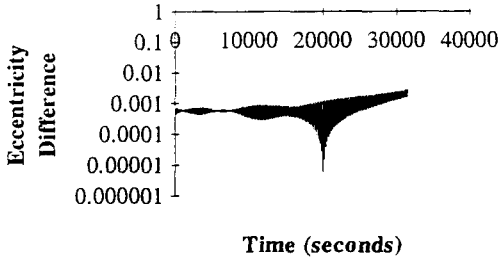


Figure 4: Absolute Value of Difference Between Numerical Approximation and Fourier Approximation vs. Time

## Inclination Control for Plane Change Maneuver for LEO-GEO Transfer

During the portion of the transfer where the inclination is changing, a Fourier series approximation on the inclination time history is done. An example time history is used to determine the associated Fourier coefficients. The superposition of these two curves is presented in Figure 5. This curve was produced using 81 Fourier coefficients (41 "c" coefficients, and 40 "d" coefficients).

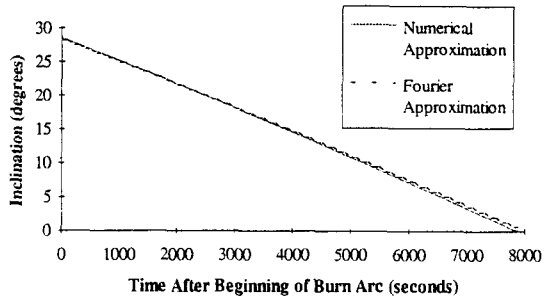


Figure 5: Inclination Time History with Fourier Series Approximation

The two curves fairly close, yet distinguishable. The absolute value of the difference between the two curves is plotted in Figure 6.

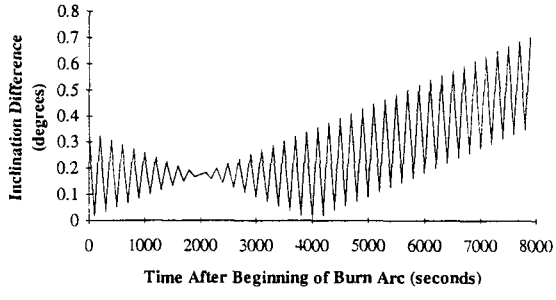


Figure 6: Absolute Value of Difference Between Numerical Approximation and Fourier Approximation vs. Time

The inclination time history approximation could be better modeled as a linear approximation, which is done in Figure 7, and the absolute value of the difference is presented in Figure 8.

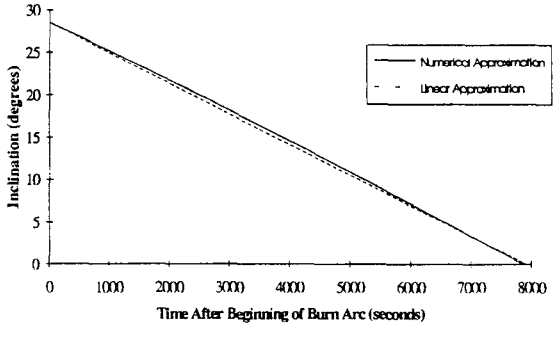


Figure 7: Inclination Time History with Linear Approximation

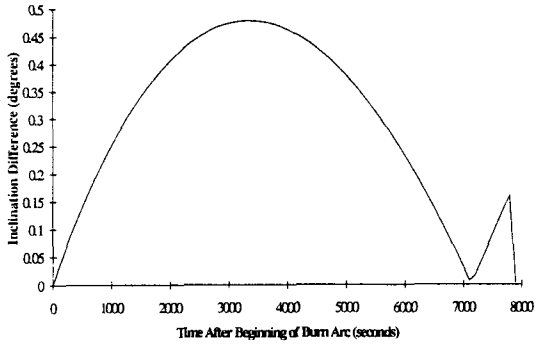


Figure 8: Absolute Value of Difference Between Numerical Approximation and Linear Approximation vs. Time

## Eccentricity Control for Recircularization for LEO-GEO Transfer

The Fourier transformation is applied to an example eccentricity time history for the recircularizing part of the results. The superposition of the Fourier series approximation on the eccentricity time history allowed for creation of Figure 9, which was created using 563 Fourier coefficients (282 "a" coefficients, and 281 "b" coefficients).

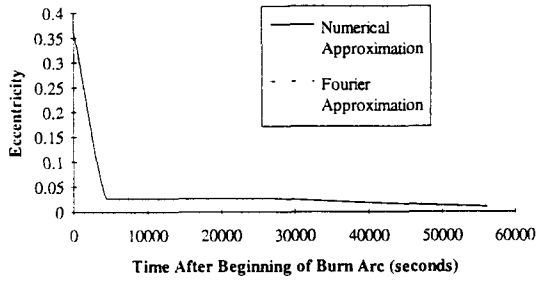


Figure 9: Eccentricity Time History with Fourier Series Approximation

The curves plotted in Figure 9, just like the others, are indistinguishable. Further discrimination of these curves plots the absolute value of the difference between these curves in Figure 10.

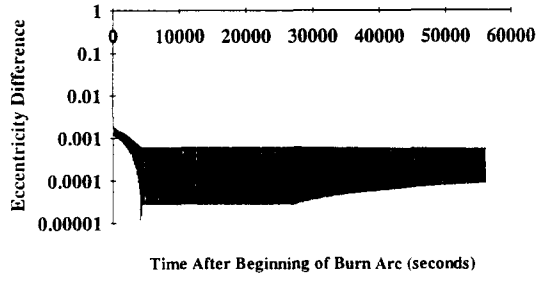


Figure 10: Absolute Value of Difference Between Numerical Approximation and Fourier Approximation vs. Time

For a more detailed discussion of the results, the reader is referred to reference 5.

## Summary, Conclusions and Further Study

This paper outlines a methodology to relax the requirement of an extensive numerical analysis of the optimal orbit transfer trajectory analysis. Simple, yet physically realizable control laws were developed, and applied to a number of initial thrust-to-mass ratios.

The equations of motion were developed in an equinoctial element frame. The general principles were developed for several control laws. A Fourier series analysis was performed on the eccentricity and inclination time histories, and the methodology was developed to describe the thrust vector control laws as a truncated Fourier series.

These control laws were pieced together to produce the transfer presented in the paper. The first burn arc was performed, and changes the apogee radius to the final, geosynchronous radius, while the perigee radius increased. When the final apogee radius was reached, a coast arc was initiated. The coast arc ended when the apogee radius was approached. At this point, the spacecraft is traveling the slowest, and therefore the out-of-plane maneuver was performed to bring the inclination down to zero. Once that was done, the orbit was recircularized, using the control law that increases the perigee radius, while keeping the apogee radius constant. The results showed that for the higher initial thrust-to-mass ratios, the cost was within a fraction of a percentage of the ideal, impulsive transfer. For the low initial thrust-to-mass ratios, the cost was about twice that of the impulsive case. In these cases, the final recircularization was performed with multiple burn arcs, each separated by a coast arc.

The Fourier series analysis technique was performed for one LEO-GEO case. Given a sufficient number of collocation points, the difference between the numerical approximation and the Fourier approximation was virtually nonexistent. A linear approximation was performed on the inclination time history, and here again, the difference was very small.

The methodology presented here was not intended as a replacement for an optimization study, but as a complement to the numerical approach. It is best used for an initial design analysis, and for spacecraft on-board guidance systems. Using the Fourier series analysis allows for a rapid reprogramming of a spacecraft with the truncated Fourier series based control law.

The most significant result shown is that this method is applicable to a seven order-of-magnitude range in initial thrust-to-mass ratios, which covers the spectrum of all orbit transfers. It is most accurate for the high initial thrust-to-mass ratios.

The results obtained from this study naturally lead to more unanswered questions. Little has been published on results for the low-thrust cases, and a numerical optimization study would be valuable to compare the results presented here with. Additionally, the initial conditions can be refined to accommodate additional constraints on the final conditions, for example, right ascension of ascending node for a LEO to GEO transfer, and development of initial launch windows characteristics for these cases.

The best comparison case to demonstrate the quality of these solutions is the ideal, impulsive case. To better compare the results, a full numerical optimization using each of the initial thrust-to-mass ratios could provide a better comparison of the results, instead of the limited results published in the literature.

Finally, an examination of the sensitivity of the Fourier approximation by a variation of the Fourier coefficients can be performed to determine how many coefficients need to be used. Furthermore, shape functions other than Fourier series approximations can be applied which could model the eccentricity and inclination with easier to construct curves.

## References


1. Broucke, R.A., and P.J. Cefola, "On The Equinoctial Orbit Elements," *Celestial Mechanics*, Vol. 5, 1972, pp. 303-310.
2. Kechichian, J.A., "Equinoctial Orbit Elements: Application to Optimal Transfer Problems," AIAA 90-2976-CP, AIAA/AAS Astrodynamics Conference, Portland, OR, August, 1990.
3. Redding, D.C., "Optimal Low-Thrust Transfers to Geosynchronous Orbit," Stanford University Guidance and Control Laboratory Report SUDAAR 539, September, 1983.
4. Spencer, D.B., and R.D. Culp. "An Analytical Solution Method for Near-Optimal, Continuous-Thrust Orbit Transfers", AAS 93-663, AAS/AIAA Astrodynamics Specialist Conference, Victoria, B.C., Canada, August, 1993.
5. Spencer, D.B., "An Analytical Solution Method for Near-Optimal, Continuous-Thrust Orbit Transfers", Ph.D. Dissertation, The University of Colorado at Boulder, January, 1994.
6. Zondervan, K.P., "Optimal Low Thrust, Three Burn Orbit Transfers With Large Plane Changes," Ph.D. Dissertation, California Institute of Technology, May, 1983.


## APPENDIX

The constituents of the matrix in equation [1], as reprinted from reference [2], are:

$$M_{11} = \frac{2a}{nr}[hk\beta\cos F - (1-h^2\beta)\sin F]$$

$$M_{12} = \frac{2a}{nr}[(1-k^2\beta)\cos F - hk\beta\sin F]$$

$$M_{13} = 0$$

$$M_{21} = \frac{G}{na^2}\left(\frac{\partial X}{\partial k} - h\beta\frac{\dot{X}}{n}\right)$$

$$M_{22} = \frac{G}{na^2}\left(\frac{\partial Y}{\partial k} - h\beta\frac{\dot{Y}}{n}\right)$$

$$M_{23} = \frac{k}{Gna^2}(qY - pX)$$

$$M_{31} = -\frac{G}{na^2}\left(\frac{\partial X}{\partial h} + k\beta\frac{\dot{X}}{n}\right)$$

$$M_{32} = -\frac{G}{na^2}\left(\frac{\partial Y}{\partial h} + k\beta\frac{\dot{Y}}{n}\right)$$

$$M_{33} = -\frac{h}{Gna^2}(qY - pX)$$

$$M_{41} = 0$$

$$M_{42} = 0$$

$$M_{43} = \frac{KY}{2Gna^2}$$

$$M_{51} = 0$$

$$M_{52} = 0$$

$$M_{53} = \frac{KX}{2Gna^2}$$

$$M_{61} = \frac{\left[-2X + G\left(h\beta\frac{\partial X}{\partial h} + k\beta\frac{\partial X}{\partial k}\right)\right]}{na^2}$$

$$M_{62} = \frac{\left[-2Y + G\left(h\beta\frac{\partial Y}{\partial h} + k\beta\frac{\partial Y}{\partial k}\right)\right]}{na^2}$$

$$M_{63} = \frac{qY - pX}{Gna^2}$$

$$X = a[(1-h^2\beta)\cos F + hk\beta\sin F - k]$$

$$Y = a[hk\beta\cos F + (1-k^2\beta)\sin F - h]$$

$$\dot{X} = \frac{a^2 n}{r}[hk\beta\cos F - (1-h^2\beta)\sin F]$$

$$\dot{Y} = \frac{a^2 n}{r}[(1-k^2\beta)\cos F - hk\sin F]$$

$$G = (1-k^2-h^2)^{1/2}$$

$$\beta = \frac{1}{1+G}$$

$$r = a(1-k\cos F - h\sin F)$$

$$K = 1 + p^2 + q^2$$

$$n = \sqrt{\frac{\mu}{a^3}}$$

$\mu \equiv$ gravitational constant

$$\frac{\partial X}{\partial h} = a\left[-(h\cos F - k\sin F)\left(\beta + \frac{h^2\beta^3}{(1-\beta)}\right) - \frac{a}{r}\cos F(h\beta - \sin F)\right]$$

$$\frac{\partial X}{\partial k} = -a\left[(h\cos F - k\sin F)\frac{hk\beta^3}{(1-\beta)} + 1 + \frac{a}{r}\sin F(\sin F - h\beta)\right]$$

$$\frac{\partial Y}{\partial h} = a\left[(h\cos F - k\sin F)\frac{hk\beta^3}{(1-\beta)} - 1 + \frac{a}{r}\cos F(k\beta - \cos F)\right]$$

$$\frac{\partial Y}{\partial k} = a\left[(h\cos F - k\sin F)\left(\beta + \frac{k^2\beta^3}{(1-\beta)}\right) + \frac{a}{r}\sin F(\cos F - k\beta)\right]$$

$$\lambda = F - k\sin F + h\cos F$$

$$\hat{u} = u_f\hat{f} + u_g\hat{g} + u_w\hat{w}$$

and

$u_f, u_g, u_w$ *are unit vector components in the* $\hat{f}, \hat{g}, \hat{w}$ *directions, respectively.*